

Local moments and magnetic correlations above the Curie temperature in thin films on and embedded in nonmagnetic substrates: Fe/Cu(100), Co/Cu(100), and Fe/W(100)

S. S. A. Razee* and J. B. Staunton

Department of Physics, University of Warwick, Coventry CV4 7AL, United Kingdom

L. Szunyogh

Department of Theoretical Physics, Budapest University of Technology and Economics, Budafoki út. 8, H-1521 Budapest, Hungary and Center for Computational Materials Science, Technical University of Vienna, Getreidemarkt 9/158, A-1060 Vienna, Austria

B. L. Györfy

H.H. Wills Physics Laboratory, University of Bristol, Tyndall Avenue, Bristol BS8 1TL, United Kingdom

(Received 21 March 2002; published 16 September 2002)

We describe a mean-field theory of magnetic fluctuations in layered metallic materials at finite temperatures. It has a first-principles electronic structure basis and uses the spin-polarized screened Korringa-Kohn-Rostoker method and the coherent-potential approximation to describe the effects of the fluctuating “local moments” upon the electronic structure. At no stage is there a fitting to an effective classical Heisenberg model. From this disordered local moment picture we find the layer dependent paramagnetic spin susceptibility of films and multilayers above the Curie temperature T_c which describes how the type of magnetic correlations varies layer by layer. We study thin films of Fe and Co (1–8 layers) on and embedded in nonmagnetic substrates, specifically bcc-Fe/W(100), fcc-Fe/Cu(100), and fcc-Co/Cu(100). In uncapped Fe/W(100) we find intralayer ferromagnetic correlations in all thicknesses of the iron film except in the layer nearest the W substrate in agreement with experiment. The interlayer couplings are also ferromagnetic and short ranged. There are also ferromagnetic intralayer and interlayer couplings throughout the Co films in fcc-Co/Cu(100). In the Fe/Cu(100) system the top two layers are coupled ferromagnetically and the rest antiferromagnetically. Cu capping has a profound effect upon the magnetic coupling in both Fe/Cu(100) and Co/Cu(100) with T_c showing an oscillating behavior as a function of the cap layer thickness. In contrast there is no dramatic effect when Fe films are embedded in W(100).

DOI: 10.1103/PhysRevB.66.094415

PACS number(s): 75.10.Lp, 75.30.Cr, 75.40.Cx, 75.50.Bb

I. INTRODUCTION

Magnetic properties of materials with two-dimensional geometry such as thin films and multilayers are very important from both fundamental and technological viewpoints.^{1,2} Epitaxial thin-film structures offer unique opportunities for exploring the relationship between structure and magnetism¹ because new phases of matter (e.g., bcc Ni, fcc Fe, fcc Co, etc.) can be stabilized as thin-film structures on suitable growth templates by molecular beam epitaxy and pulsed laser deposition techniques.³ During the last decade considerable theoretical and experimental progress has been made towards understanding the metallic magnetism of bulk as well as these two-dimensional systems at zero temperature. Well below the Curie temperature T_c , magnetic properties of ferromagnetic materials, pure elements, ordered, and disordered alloys alike, are well explained from first-principles electronic structure calculations. But at higher temperatures, above T_c for example, the effects of thermally induced spin fluctuations or “local moments” need to be incorporated into the electronic description. We address this issue in this paper.

Most theoretical work^{4–7} on metallic magnets at finite temperature assumes a separation between fast and slow motions of the interacting many electron system. For times τ long in comparison to electronic hopping times \hbar/W ($\approx 10^{-15}$ sec), where W is the relevant bandwidth, but short compared to some characteristic spin fluctuation times, the

spin orientations of the electrons leaving an atomic site are sufficiently correlated with those arriving that a nonzero magnetization exists when the appropriate quantity is averaged over τ . These are the “local magnetic moments” on each site and are oriented in arbitrary directions $\{\mathbf{e}_i\}$ above T_c giving a net zero magnetization on the whole. The local moments change their orientations on the longer time scale while their magnitudes fluctuate rapidly on the time scale τ . Below T_c , on the average, the moments align themselves to produce ferromagnetic or antiferromagnetic order overall. Within the nonrelativistic spin-polarized Korringa-Kohn-Rostoker (KKR) method, the disordered local moment (DLM) model above T_c maps onto a problem of a disordered equiatomic binary alloy $A_{0.5}B_{0.5}$ with A and B components representing sites with “up” and “down” moments⁸ respectively. Therefore, one can use the well-defined tools of the KKR coherent-potential approximation (CPA) to solve this problem. Also, by allowing inhomogeneous magnetic fluctuations at all sites in the system, and determining their response to a “small” site-dependent external magnetic field $\{\mathbf{h}_i\}$, the temperature dependence of magnetic correlations and the transition to a magnetically ordered state can be investigated. Using this approach, Staunton *et al.*⁹ have derived an expression for the paramagnetic spin susceptibility. This approach has been very successful in explaining the magnetic correlations in the paramagnetic state of several

magnetic metals and alloys as well as determining the T_c 's.^{9–12}

One of the earliest predictions of the DLM theory implemented within the KKR-CPA scheme for bulk materials was that a “local exchange splitting” should be evident in the electronic structure of the paramagnetic state.^{10,11} This means that an electron with spin parallel to a local moment will have a different density of states (DOS) to that of an electron with spin antiparallel. Of course, when an average over all the orientations of the moments in the paramagnetic state is taken it is inevitable that the electronic structure does not have any spin-polarization overall. But the consequences of the presence of the fluctuating local moments can still be identified, both theoretically and experimentally. This local exchange splitting is the cause of local moment formation. These qualitative features have been observed in photoemission¹³ and inverse photoemission¹⁴ spectra measurements of bcc Fe.

We have recently outlined a first-principles electronic structure based DLM theory for thin films and multilayers¹⁵ within the screened KKR-CPA approach^{16–19} and have studied the onset of magnetic order in fcc-Fe thin films on Cu(100) substrate finding good agreement with rich experimental data.^{20,21} We found that the features of DLM theory observed in the bulk solids, in particular the local exchange splitting and the existence of local moments, now pick up a layer dependence. Consequently, the magnetic interactions can vary layer by layer and also depend strongly on the depth at which the films are embedded in the substrate. Moreover the thickness of the cap on the films affects the magnetic ordering transition temperatures. In particular, for Cu-capped Fe/Cu(100) (Ref. 15) we found that the T_c depends strongly on the film thickness and oscillates as a function of the thickness of the capped layer in very good agreement with experimental observations.²⁰

In this paper, we describe our scheme in some detail and describe the results for fcc-Co thin films on Cu(100) and compare them with our results for fcc-Fe/Cu(100). We also examine the onset of magnetic order in thin bcc-based Fe films on a W(100) substrate. The films range from 1 to 8 monolayers in thickness. A common feature that we find for all three systems is that of the local moment in the top layer being about 10–15 % larger than that of the layer adjacent to the substrate. The Curie temperature of a single monolayer of Co/Cu(100) is 1091 K in our mean field approximation and it steadily decreases with the increase in film thickness, approaching the Curie temperature of the bulk fcc-Co for the same lattice parameter. The effective “exchange interactions” of the fcc-Co/Cu(100) system are long ranged as in the fcc-Fe/Cu(100) system, but unlike the latter system, the magnetic interactions are always ferromagnetic, even capping by Cu overlayers does not alter this aspect of the magnetic interactions. However, in the bcc-Fe/W(100) system the intralayer magnetic interactions in the layer adjacent to the substrate are antiferromagnetic while all other interactions are ferromagnetic. The effective “exchange interactions” are very small after the first-nearest-neighbor layer. The Curie temperature of Fe₂/W(100) system is 969 K and increases monotonically with the film thickness and for thick films it

reaches the value of the bulk bcc-Fe for the same lattice parameter.

Recently 2D effective Heisenberg models for single Fe and Co monolayers on and embedded in Cu(100) were constructed by Pajda *et al.*²² They used exchange interactions extracted from *ab initio* calculations of the spin wave spectra of the metals' low-temperature ferromagnetic phases and a small anisotropy energy parameter was added to the models. As expected for 2D systems they found the T_c 's to be substantially reduced when a more sophisticated approximation based on the random phase approximation was used in preference to a mean-field treatment (MFT). They also found an oscillatory behavior of the T_c 's with Cu-capping thickness in both approximations. Interestingly although our DLM approach requires no similar mapping to an effective Heisenberg model our T_c 's of single Fe and Co layers on Cu(100) of 1224 and 1091 K, respectively, are rather comparable to the Pajda *et al.* MFT estimates of 1068 and 1043 K.²² Note, however, our calculations contain an account of the electronic structure which supports and which is affected by the magnetic fluctuations.

It is well known that Mermin-Wagner theorem²³ forbids a 2D Heisenberg model to have magnetic long-range order. We can presume that in a nonrelativistic electronic theory such as ours that a similar principle is also valid implying that any instability of the paramagnetic state of the monolayer found from our mean field theory calculations cannot be taken as a precursor to magnetic long-range order. In a relativistic version of our calculations, however, we can expect a crossover to an Ising-like universality class on account of spin-orbit coupling and dipolar interactions introducing magnetic anisotropic effects. Thus, although our calculated mean field theoretical T_c 's are likely to be overestimates, they can be taken as indicative of what will happen in a more complete theory. Also, it is reasonable to assume that the magnetic intralayer and interlayer interactions, determined by the electronic structures of their DLM paramagnetic states, are reasonably well described by our MFT.

The outline of the paper is as follows. In Sec. II, we briefly review the theoretical framework of the DLM picture and describe its extension to layered systems. The following section contains computational details and in Sec. IV we present and discuss our results, finishing with a summary and conclusions in Sec. V.

II. THEORETICAL FRAMEWORK

We start from the key assumption of a separation between fast and slow electronic degrees of freedom in a metallic magnet. The consequence is that “local moments” are set up by the collective behavior of the interacting electrons and their orientations fluctuate relatively slowly. To make headway with this simple picture we specify a particular arrangement of local moment orientations by $\{\mathbf{e}_i\}$ and propose that the long time averages can be evaluated with respect to the ensemble of these orientational configurations. The probability of finding a particular orientational configuration $\{\mathbf{e}_i\}$ at a given temperature T is given by the Gibbsian measure

$$P(\{\mathbf{e}_i\}) = Z^{-1} \exp[-\beta\Omega(\{\mathbf{e}_i\})],$$

where the partition function is given by

$$Z = \prod_j \int d\mathbf{e}_j \exp[-\beta\Omega(\{\mathbf{e}_j\})].$$

Here, $\Omega(\{\mathbf{e}_j\})$ is the ‘‘generalized’’ electronic grand potential adapted from spin density functional theory and $\beta = (k_B T)^{-1}$, k_B being the Boltzmann constant.^{10,12} Evidently, $\Omega(\{\mathbf{e}_j\})$ plays the role of a classical ‘‘spin’’ Hamiltonian. The free energy associated with the orientational fluctuations and also the creation of particle-hole pairs is $F = -\beta^{-1} \ln Z$. By expanding $\Omega(\{\mathbf{e}_j\})$ about a suitably chosen single-site reference ‘‘spin’’ Hamiltonian $\Omega_0(\{\mathbf{e}_i\}) = \sum_i \omega_i(\mathbf{e}_i)$ and using the Feynman-Peierls’ inequality,²⁴ a mean-field theory is set up. The probability distribution function for the reference state is $P_0(\{\mathbf{e}_i\}) = \prod_i P_0(\mathbf{e}_i)$, where $P_0(\mathbf{e}_i)$ is the probability of finding the moment on the i th site oriented along \mathbf{e}_i ,

$$P_0(\mathbf{e}_i) = \frac{\exp[-\beta\omega_i(\mathbf{e}_i)]}{\int d\mathbf{e}_i \exp[-\beta\omega_i(\mathbf{e}_i)]},$$

with $\omega_i(\mathbf{e}_i)$ given by

$$\omega_i(\mathbf{e}_i) = \prod_{j \neq i} \int d\mathbf{e}_j P_0(\mathbf{e}_j) \Omega_0(\{\mathbf{e}_k\}).$$

The magnetization per site \mathbf{M}_i is $\int d\mathbf{e}_i \mu_i(\mathbf{e}_i) \mathbf{e}_i P_0(\mathbf{e}_i)$ where $\mu_i(\mathbf{e}_i)$ is the magnitude of the local moment orientated along the unit vector \mathbf{e}_i on a site i . Above T_c , ω_i and $P_0(\mathbf{e}_i)$ are independent of \mathbf{e}_i and the moments have the same probability of being oriented in any direction, i.e., $\mathbf{M}_i = 0$. With this symmetry the problem can be mapped onto a random binary alloy $A_{0.5}B_{0.5}$ with A and B species representing ‘‘up-spin’’ and ‘‘down-spin’’ sites^{10,11} and we can apply the first-principles electronic structure schemes, such as the self-consistent field KKR-CPA, developed originally for disordered alloys.

Following Ref. 9 we investigate the response of the DLM paramagnetic state to the application of a small, external magnetic field $\{\mathbf{h}_i\}$ which can vary from site to site. Focusing on the dominant response of the system to line up the moments with the applied field, we obtain the following expression for the paramagnetic spin susceptibility, which for a general set of sites can be written as

$$\chi_{ij} = \frac{\beta}{3} \mu_i^2 \delta_{ij} + \frac{\beta}{3} \sum_k S_{ik}^{(2)} \chi_{kj}. \quad (2.1)$$

In this equation, μ_i is the magnitude of the local magnetic moment on the i th site, and the direct correlation functions

$$S_{ik}^{(2)} = - \left. \frac{\partial^2 \bar{\Omega}}{\partial m_i \partial m_k} \right|_{\{m_i = \bar{m}_i\}},$$

where $m_i = \langle \mathbf{e}_i \rangle$, related to the magnetization \mathbf{M}_i in site i , and $\bar{\Omega}$ is the averaged Grand potential $\int d\mathbf{e}_i \omega_i(\mathbf{e}_i) P_0(\mathbf{e}_i)$.

In films and multilayers there is intralayer two-dimensional translational symmetry so that the magnitudes of the local moments, $\{\mu_{ij}\}$ of the paramagnetic DLM state can vary in different layers, while being identical in a par-

ticular layer. By choosing the sites i and j to lie in the layers denoted by P and Q respectively, Eq. (2.1) can be rewritten as

$$\chi_{PiQj} = \frac{\beta}{3} \mu_{Pi}^2 \delta_{PQ} \delta_{ij} + \frac{\beta}{3} \sum_{Sk} S_{PiSk}^{(2)} \chi_{SkQj}, \quad (2.2)$$

where the combination $\{Pi\}$ indicates that the site i is in layer P . In the two-dimensional geometry, the direct correlation function $S_{PiSk}^{(2)}$ can be written as

$$S_{PiSk}^{(2)} = - \frac{Im}{\pi} \int_{-\infty}^{\infty} d\varepsilon f(\varepsilon, \nu) Tr[\{(X_{\uparrow}^P)^{-1} - (X_{\downarrow}^P)^{-1}\} \\ \times \{\lambda^{PiSk} - (X_{\uparrow}^P - X_{\downarrow}^P) \delta_{PS}^{ik}\}],$$

where

$$\lambda^{PiSk} = \delta_{PS}^{ik} (X_{\uparrow}^P - X_{\downarrow}^P) - X_{\uparrow}^P \left[\sum_{Qm} \tau^{PiQm} \lambda^{QmSk} \tau^{QmPi} \right. \\ \left. - \tau^{PiPi} \lambda^{PiSk} \tau^{PiPi} \right] X_{\downarrow}^P.$$

In these expressions τ^{PiQj} are the ‘‘CPA’’ path-operator matrices in a layer and site representation $t_{\uparrow(\downarrow)}^P$ is the scattering matrix for the up (down) site, and t is the scattering matrix for the CPA effective medium. $f(\varepsilon, \nu)$ is the Fermi factor with chemical potential ν and the trace is over the angular momentum indices. The up-arrow (\uparrow) and down-arrow (\downarrow) refer to the up sites and down sites, respectively. Note that, the scattering matrices t_{\uparrow}^P , t_{\downarrow}^P , and t^P as well as the ‘‘extra’’ scattering from ‘‘up’’ (‘‘down’’) sites, $X_{\uparrow(\downarrow)}^P$ are layer dependent, i.e.,

$$X_{\uparrow(\downarrow)}^P = [\{(t_{\uparrow(\downarrow)}^P)^{-1} - (t^P)^{-1}\}^{-1} + \tau^{P0P0}]^{-1} \quad (2.3)$$

and satisfy the KKR-CPA condition

$$X_{\uparrow}^P + X_{\downarrow}^P = 0$$

for each layer separately.²⁵ We can take a 2D lattice Fourier transform of Eq. (2.2), obtaining,

$$\chi_{PQ}(\mathbf{q}_{\parallel}) = \sum_{ij} \chi_{PiQj} \exp[-i\mathbf{q}_{\parallel} \cdot (\mathbf{R}_i - \mathbf{R}_j)] \\ = \frac{\beta}{3} \mu_P^2 \delta_{PQ} + \frac{\beta}{3} \sum_S S_{PS}^{(2)}(\mathbf{q}_{\parallel}) \chi_{SQ}(\mathbf{q}_{\parallel}), \quad (2.4)$$

where \mathbf{q}_{\parallel} is a wave vector in any layer. Note that, the local magnetic moment μ_P is same on each site in the P th layer, because of two-dimensional translational symmetry. $S_{PS}^{(2)}(\mathbf{q}_{\parallel})$ is given by

$$S_{PS}^{(2)}(\mathbf{q}_{\parallel}) = - \frac{Im}{\pi} \int_{-\infty}^{\infty} d\varepsilon f(\varepsilon, \nu) Tr[\{(X_{\uparrow}^P)^{-1} - (X_{\downarrow}^P)^{-1}\} \\ \times \{\lambda^{PS}(\mathbf{q}_{\parallel}) - (X_{\uparrow}^P - X_{\downarrow}^P) \delta_{PS}\}], \quad (2.5)$$

where

$$\begin{aligned} \lambda^{PS}(\mathbf{q}_{\parallel}) = & \delta_{PS}(X_{\uparrow}^P - X_{\downarrow}^P) - X_{\uparrow}^P \left[\frac{1}{S_{\text{BZ}}} \int d^2\mathbf{k}_{\parallel} \sum_Q \tau^{PQ}(\mathbf{k}_{\parallel} + \mathbf{q}_{\parallel}) \right. \\ & \left. \times \lambda^{QS}(\mathbf{q}_{\parallel}) \tau^{QP}(\mathbf{k}_{\parallel}) - \tau^{P0P0} \lambda^{PS}(\mathbf{q}_{\parallel}) \tau^{P0P0} \right] X_{\downarrow}^P \end{aligned} \quad (2.6)$$

and S_{BZ} is the area of the 2D Brillouin zone with wave vectors \mathbf{k}_{\parallel} inside. The most difficult part of the whole procedure is the convolution integral in Eq. (2.6) together with the solution of this equation. In principle, Eq. (2.6) can be solved by either considering it as a set of ‘‘linear’’ equations or alternatively, by an iterative approach starting with $\lambda^{QS}(\mathbf{q}_{\parallel}) = \delta_{QS}(X_{\uparrow}^Q - X_{\downarrow}^Q)$. Both these approaches are computationally intensive. In our studies on the effect of compositional order on the magnetocrystalline anisotropy^{26,27} of transition metal alloys, we have found that, normally, the first iteration is quite sufficient.

Once we have evaluated $S_{PS}^{(2)}(\mathbf{q}_{\parallel})$, we can determine $\chi_{PQ}(\mathbf{q}_{\parallel})$ by Eq. (2.4). Equation (2.4) can be viewed as a matrix equation in layer-space, i.e., $\chi(\mathbf{q}_{\parallel}) = (\beta/3)\mu^2 + (\beta/3)S^{(2)}(\mathbf{q}_{\parallel})\chi(\mathbf{q}_{\parallel})$ (μ is a diagonal matrix with elements μ_P) from which $\chi(\mathbf{q}_{\parallel})$ can be obtained. The transition temperature will be given by the condition that $\|\chi^{-1}(\mathbf{q}_{\parallel}^{\text{max}})\| = 0$, where $\mathbf{q}_{\parallel}^{\text{max}}$ is the wave vector for which the matrix $S^{(2)}(\mathbf{q}_{\parallel})$ has the largest positive eigenvalue. $\mathbf{q}_{\parallel}^{\text{max}} = 0$ for the three systems studied in this paper [except the Fe monolayer on W(100)] and the Curie temperature T_c is obtained by solving

$$\|3k_B T_c I - S^{(2)}(\mathbf{q}_{\parallel} = 0)\| = 0.$$

When the system is cooled down from its paramagnetic state at high temperatures, the magnetic order will start around the temperature at which the instabilities in the spin-fluctuations diverge. In our MFT this occurs at the temperature corresponding to a third of largest positive eigenvalue of $S^{(2)}(\mathbf{q}_{\parallel} = 0)$.

$$T_c = \frac{\text{Largest positive eigenvalue of } S^{(2)}(\mathbf{q}_{\parallel} = 0)}{3k_B}. \quad (2.7)$$

It is also evident from Eq. (2.4) that the χ_{PQ} 's are likely to follow a Curie-Weiss law as a function of temperature.

We have used the screened KKR method^{16–18} in all our calculations and it is straightforward to see that the form of Eqs. (2.5) and (2.6) remains unchanged under the screening transformation, i.e., the actual t matrices and the path-operator matrices are related to those in the screened representation as²⁸

$$t = t^{\alpha} + \alpha,$$

$$\tau = t(t^{\alpha})^{-1} \tau^{\alpha} (t^{\alpha})^{-1} t - t(t^{\alpha})^{-1} \alpha,$$

where α is the matrix of energy-dependent screening parameters, and the matrices with superscript α are in the screened representation.

III. COMPUTATIONAL DETAILS

We have used the spin-polarized screened KKR method^{16–18} for layered systems²⁸ in all our calculations. The electronic structures of the paramagnetic DLM states of Fe_n ($n \leq 8$) on W(001) and Cu(001) substrates and Co_n ($n \leq 8$) on Cu(001) substrate were calculated self-consistently within the local spin density functional theory.²⁹ We have constrained the lattice constants of the films to be the same as that of the substrate, i.e., we have neglected the effects of lattice strain on the electronic structure. For fcc-Fe and fcc-Co films on and embedded in Cu(100) we have used the lattice constant of fcc-Cu (6.83 a.u.), and for bcc-Fe films on and in W(100), the lattice constant of the bcc-W (5.98 a.u.). For each n , the electronic structure of the DLM state was calculated self-consistently using 78 k_{\parallel} points in the irreducible part of the surface Brillouin zone. The DLM state is described using the CPA for the layered systems as outlined in Ref. 25. In all the cases, a buffer of three layers of the substrate as well as a buffer of three (at least) layers of vacuum was calculated self-consistently along with the potentials on each layer. The self-consistent layer-resolved potentials were then used to calculate the DOS and local magnetic moments on each layer as well as the layer-dependent effective ‘‘exchange parameters’’ for $\mathbf{q}_{\parallel} = 0$.

As an alternative to carrying out the computationally intensive convolution integrals and also making approximations in Eqs. (2.5), (2.6), for $S^{(2)}(\mathbf{q}_{\parallel} = 0)$ we consider

$$S_{PQ}^{(2)}(\mathbf{q}_{\parallel} = 0) = \sum_{i \in P} \sum_{j \in Q} S_{PiQj}^{(2)} \quad (3.1)$$

we consider the application of a local small external uniform magnetic field to every site j in layer Q which induces a change in the total ‘‘Weiss’’ field of layer P , $\Delta S_P^{(1)}$. This can be written in terms of the $S_{PiQj}^{(2)}$'s as follows:

$$\Delta S_P^{(1)} = \sum_{i \in P} \Delta S_{Pi}^{(1)} = - \sum_{i \in P} \sum_{j \in Q} S_{PiQj}^{(2)} \Delta m_{Qj}, \quad (3.2)$$

where Δm_{Qj} is the induced magnetization on the site $j \in Q$. This is the same for each site and $\Delta m_{Qj} = \Delta m_Q$ for all $j \in Q$, describing a uniform magnetization on a particular layer. Therefore, with the help of Eq. (3.1), we can rewrite Eq. (3.2) as

$$\Delta S_P^{(1)} = - \sum_Q S_{PQ}^{(2)}(\mathbf{q}_{\parallel} = 0) \Delta m_Q. \quad (3.3)$$

In particular, if we consider the magnetization change on one layer only, say Q , then we obtain

$$S_{PQ}^{(2)}(\mathbf{q}_{\parallel} = 0) = - \frac{\Delta S_P^{(1)}}{\Delta m_Q}. \quad (3.4)$$

Therefore, by calculating the changes in the total ‘‘Weiss’’ field $\Delta S_P^{(1)}$ on different layers induced by a small change in the magnetization Δm_Q on a particular layer Q we can generate $S_{PQ}^{(2)}(\mathbf{q}_{\parallel} = 0)$ for $P = 1 \cdot \cdot \cdot n$ (where n is the total number of layers). By following the same procedure for different Q 's

TABLE I. Local magnetic moments on different layers and the Curie temperatures of the $\text{Co}_n/\text{Cu}(100)$ system. The layer L_1 is adjacent to the substrate and layer L_n is the topmost layer.

n	Local magnetic moments (μ_B)								T_c (K)
	L_1	L_2	L_3	L_4	L_5	L_6	L_7	L_8	
1	1.66								1091
2	1.39	1.59							939
3	1.38	1.21	1.63						891
4	1.39	1.21	1.26	1.63					919
5	1.40	1.21	1.26	1.26	1.63				965
6	1.40	1.21	1.26	1.26	1.25	1.63			973
7	1.40	1.21	1.26	1.26	1.26	1.25	1.63		977
8	1.40	1.21	1.26	1.26	1.26	1.26	1.25	1.63	975
Bulk	1.26								965

we can generate all the $S_{PQ}^{(2)}(\mathbf{q}_{\parallel}=0)$ for the system. Calculation of $S_p^{(1)}$ is obtained from Ref. 10

$$S_p^{(1)} = -\frac{\text{Im}}{\pi} \int_{-\infty}^{\infty} d\varepsilon f(\varepsilon, \nu) [\ln \|D_{\uparrow}^P\| - \ln \|D_{\downarrow}^P\|], \quad (3.5)$$

where

$$D_{\uparrow(\downarrow)}^P = [I + \{(t_{\uparrow(\downarrow)}^P)^{-1} - (t^P)^{-1}\} \tau^{P0P0}]^{-1}.$$

One can then calculate $S_p^{(1)}$ for different layers by introducing a very small change in the local magnetization at a particular layer, and from that, generate a set of linear equations involving $S_{PQ}^{(2)}(\mathbf{q}_{\parallel}=0)$ using Eq. (3.4). These equations then can be solved to obtain $S_{PQ}^{(2)}(\mathbf{q}_{\parallel}=0)$. In this paper we report results from this approach. We are restricted to systems where $S_{PQ}^{(2)}(\mathbf{q}_{\parallel})$ is greatest for $\mathbf{q}_{\parallel}=0$, i.e., we can explore only the possibility of transition into states with ferromagnetic order within each plane although the layers themselves may be ferromagnetically or antiferromagnetically coupled. From these values of $S_{PQ}^{(2)}(\mathbf{q}_{\parallel}=0)$ one can then obtain the T_c from Eq. (2.7) as well as the susceptibility $\chi_{PQ}(\mathbf{q}_{\parallel}=0)$ from Eq. (2.4).

IV. RESULTS

A. fcc Co/Cu(100) and Cu/Co/Cu(100)

Co/Cu(100) is ideal for the study of magnetism in systems with reduced dimension owing to the rather small lattice mismatch (about 2%) and the complete immiscibility of the constituent materials in the bulk phase³⁰ so that a Co film grows layer by layer on a Cu(100) substrate with little interfacial roughness.³¹ Co films on Cu(100) grow in an fcc-like structure with slight tetragonal distortion (compression) and this structure persists up to a large thickness.³² Due to a mismatch between the Co and Cu bands across the interface, multilayers of Co and Cu exhibit a giant magnetoresistance ratio^{33,34} and form a part of many spin-valve elements, such as those used in read heads of magnetic storage devices.³⁵ Unlike some other ferromagnetic films on nonmagnetic sub-

strates the equilibrium direction of magnetization always lies in the plane of the film in the Co/Cu(100) system.^{32,36}

Willis and co-workers^{37,38} have determined the Curie temperatures of Co/Cu(100) systems as a function of film thickness by using the surface magneto-optic Kerr effect. They find that the Curie temperatures follow a thickness-dependent scaling law

$$\frac{1}{T_c(n)} = \frac{1}{T_c(\infty)} \left[1 + \left(\frac{n_0}{n-n'} \right)^\lambda \right], \quad (4.1)$$

where n is the number of monolayers in the film and n_0 , n' , and λ are material-dependent parameters ($n_0 \approx 1.8$, $n' = 1$, and $\lambda \approx 1$). This phenomenological behavior implies that $T_c = 0$ for a single monolayer and increases monotonically with film thickness. However, it is found that as the films become ultrathin they are no longer homogeneous and uniformly thick, but begin to break up into islands of varying thickness. This might be the reason that experiment finds the magnetization and T_c to decrease as the films' thicknesses are reduced and to vanish in the single monolayer limit.

We have calculated the magnetic properties of the fcc- $\text{Co}_n/\text{Cu}(100)$ ($n \leq 8$) system above T_c within our mean field DLM theory. The local moments on each layer and the corresponding T_c 's along with the results for the bulk fcc-Co for the same lattice parameter are presented in Table I. The local moment on the topmost layer is about 15% larger than that on the layer adjacent to the substrate, whilst the moments in the interior layers of the thicker films are very close to those of the bulk fcc-Co for the same lattice parameter. The T_c for the single monolayer is quite high, significantly overestimated by our MFT,²² and in contrast to experimental observations, this steadily decreases as the number of layers is increased and stabilizes around the value of the bulk for layers $n \geq 7$. We present the effective "exchange parameters" $S_{PQ}^{(2)}(\mathbf{q}_{\parallel}=0)$ for the $\text{Co}_7/\text{Cu}(100)$ system in Table II. We observe that both the interlayer as well as the intralayer, are positive implying that the magnetic correlations are ferromagnetic for all the layers in the film and that there is sig-

TABLE II. $S_{PP}^{(2)}(\mathbf{q}_{\parallel}=0)$ and interlayer $S_{PQ}^{(2)}(\mathbf{q}_{\parallel}=0)$ ($P \neq Q$) effective “exchange interactions” in meV in the uncapped $\text{Co}_7/\text{Cu}(100)$ system with the values for the $\text{Co}_3/\text{Cu}(100)$ system given in parentheses for comparison. The layer L_1 is adjacent to the $\text{Cu}(100)$ substrate and layer L_7 (L_3) is the topmost layer.

Layers	L_1	L_2	L_3	L_4	L_5	L_6	L_7
L_1	121(118)	93.7 (93.7)	-9.4(-21.1)	2.1	1.0	0.0	-0.1
L_2	93.7 (93.7)	70.1 (58.7)	84.7(103)	-4.3	1.2	0.5	0.0
L_3	-9.4(-21.1)	84.7 (103)	75.0(148)	92.2	-4.1	1.2	0.8
L_4	2.1	-4.3	92.2	75.4	92.1	-4.7	4.5
L_5	1.0	1.2	-4.1	92.1	76.1	91.0	-9.6
L_6	0.0	0.5	1.2	-4.7	91.0	60.7	111.9
L_7	-0.1	0.0	0.8	4.5	-9.6	112	155

nificant magnetic interactions up to third nearest-neighbor layers. This qualitative behavior is found for all the films.

In the fcc-Fe/Cu(100) system, which we have studied in a previous paper¹⁵ and show some further results in the next section, a marked change in the magnetic properties occurs when the Fe film is embedded into the Cu substrate. In particular, the T_c showed an oscillating behavior as a function of capping layer thickness which was also found in experiment.^{20,15} We carried out a similar investigation for the Co/Cu(100), calculating the magnetic properties of the $\text{Cu}_m/\text{Co}_n/\text{Cu}(100)$ systems and show in Fig. 1 results for 3 and 7 ML thick Co films ($n=3$ and 7) capped by $m=1,2,3,4$, and 5 ML's of Cu. In contrast to Fe/Cu(100), the capping does not change the sign of $S_{PQ}^{(2)}(\mathbf{q}_{\parallel}=0)$, i.e., the interlayer magnetic correlations remain ferromagnetic even after capping, although the T_c is also altered profoundly as a function of cap-layer thickness. For the $\text{Co}_3/\text{Cu}(100)$ system a single Cu cap layer suppresses the T_c quite drastically by more than 200 K while the second cap layer increases it by about 140 K. The third cap layer reduces the T_c but only slightly (20 K) unlike the Fe/Cu(100) system¹⁵ and further cap layers do not cause any oscillations in T_c rather they have a steadying effect. Therefore, for thick Cu overlayers the T_c is around 800 K for this system. To our knowledge there are no experimental results on the capped fcc-Co/Cu(100) system. The $\text{Co}_7/\text{Cu}(100)$ films show a similar behavior but the suppression of T_c by the second cap layer is only by about 60 K and for thicker overlayers the T_c stabilizes at a much higher value of 920 K.

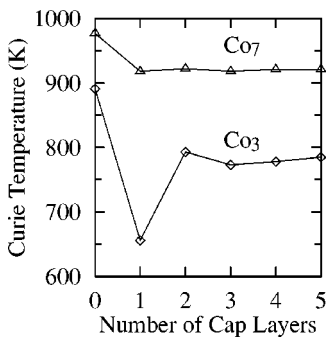


FIG. 1. Curie temperatures of the $\text{Cu}_m/\text{Co}_3/\text{Cu}(100)$ and $\text{Cu}_m/\text{Co}_7/\text{Cu}(100)$ systems for different Cu overlayer thickness n .

To understand the electronic origin of the effect of capping on the T_c we show the electronic DOS in the topmost Co layer of the $\text{Co}_3/\text{Cu}(100)$ system as well as in the topmost Co layer of the $\text{Cu}_1/\text{Co}_3/\text{Cu}(100)$ system in Fig. 2. The Cu overlayer alters the electronic structure of the topmost Co layer in the same way as it does to that of the topmost Fe layer in the $\text{Cu}_1/\text{Fe}_3/\text{Cu}(100)$ system,¹⁵ namely, some of the electrons with spin antiparallel to the local moment on a site are transferred from the vicinity of the Fermi energy to the bottom of the band thereby reducing the “local” exchange-splitting of the paramagnetic DLM state. Also, the energy band of the electrons with spin parallel to the local moment is somewhat broadened because of the capping. This effect reduces the T_c . But unlike in the $\text{Cu}_1/\text{Fe}_3/\text{Cu}(100)$ system¹⁵ it does not switch the magnetic interactions between the layers to antiferromagnetic because the peak in the band of the electrons with spin antiparallel to the local moment is very close to the Fermi energy which makes the band partially filled rather than half filled.

B. fcc Fe/Cu(100) and Cu/Fe/Cu(100)

Ultrathin fcc Fe films on and embedded in Cu(100) represent one of the most challenging and rich magnetic systems

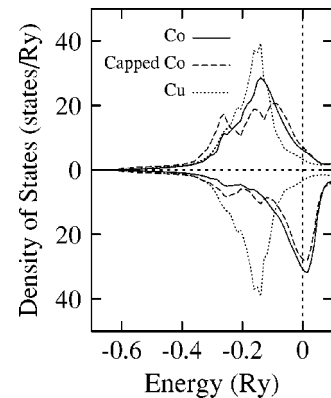


FIG. 2. Electronic density of states (DOS) in the topmost Co layer of the $\text{Co}_3/\text{Cu}(100)$ system. The full line represents the uncapped system whilst the dashed line is for the system capped with a single monolayer of Cu. The dotted line represents the capping Cu layer. The upper (lower) half of the figure shows the DOS for an electron spin-polarized parallel (antiparallel) to the local moment on a site. The energy is measured from the Fermi energy.

because of their complex, yet interesting, structural, and magnetic properties.^{39,40,21} While thick Fe films on Cu(100) grown at room temperature exist in a thermodynamically stable bcc structure, for films with thickness less than 11 monolayers fcc Fe films with both ferromagnetic high spin and antiferromagnetic low spin behavior are observed.^{41,42} Films with thickness less than 5 monolayers exhibit a homogeneous magnetization,^{43,44} however for the thickness range between 5 and 11 monolayers, only the top two surface layers are apparently ferromagnetically coupled.^{21,43} The inner layers of 6–11 monolayer-thick films seem to be in the type-I antiferromagnetic phase (CuAu-type structure) in which the layers, which themselves are ferromagnetic, are coupled antiferromagnetically.^{45,46}

Recently,¹⁵ we calculated the “exchange parameters” of the fcc-Fe_{*n*}/Cu(100) system ($n \leq 8$) from first-principles electronic structure calculations as described in this paper and our results indeed showed that only the first two layers to be ferromagnetically linked with all the subsequent layers coupled antiferromagnetically. We also calculated the T_c 's of this system as a function of film thickness which showed a monotonically decreasing behavior as a function of film thickness before stabilizing to a value of 485 K for thicker films. Following the fascinating discovery by a recent experiment²⁰ using the magneto-optical Kerr effect that the T_c of a copper-capped Fe film shows an unusual oscillatory behavior as a function of the Cu overlayer thickness we found from our calculations of this effect that it is not predominantly a consequence arising from the tetragonal distortion of the film²⁰ but instead is related to a change in the electronic structure of Fe and Cu layers near the interface alone. Our calculated values of T_c 's for embedded Fe films in Cu(100) substrate¹⁵ indeed showed an oscillatory behavior as a function of overlayer thickness in excellent agreement with the experimental observations. Our neglect of the lattice mismatch effects gives credence to above suggestion that this effect is entirely due to the hybridization of Fe and Cu states at and near the interface.

Results of our calculations of T_c and $S_{PQ}^{(2)}(\mathbf{q}_{\parallel}=0)$ for Fe films for a range of thicknesses ($n \leq 8$) on and embedded in Cu(100) are presented in Ref. 15. Here we add a few further remarks concerning the magnetic correlations and spin susceptibility as a function of film and overlayer thickness. In Fig. 3 we show the layer-diagonal paramagnetic spin susceptibility $\chi_{PP}(\mathbf{q}_{\parallel}=0)$ of different layers of the Fe₇/Cu(100) system as a function of temperature. Layer L_1 is adjacent to the substrate, and layer L_7 is the top-most layer adjacent to the vacuum. It is evident that the magnetic correlations within the inner layers (layers L_2 to L_5) are very similar which is also evident from the local moments on each layer.¹⁵ However, this changes when the film is embedded. In Fig. 4 we show the layer-diagonal spin susceptibility for the topmost layer L_7 as a function of Cu cap thickness. We see that the first overlayer changes the magnetic behavior quite drastically, a two layer cap restores T_c and then more overlayers stabilize the magnetic behavior making it more similar to an Fe sandwich between two Cu substrates which has a calculated T_c of 430 K.

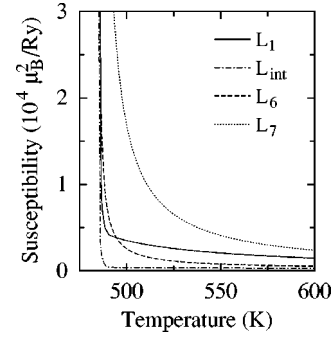


FIG. 3. Layer-diagonal paramagnetic spin susceptibility $\chi_{PP}(\mathbf{q}_{\parallel}=0)$ for different layers of the Fe₇/Cu(100) system as a function of temperature. The layer L_{int} implies the interior layers (L_2 to L_5) for which the susceptibility curves fall on each other on this scale.

C. bcc Fe/W(100) and W/Fe/W(100)

Perhaps the most obvious thin film system to study in the context of metallic magnetism is comprised of bcc-coordinated Fe. The transition from 2D to 3D bulk behavior can be tracked. Experimentally this can be realized by the investigation of Fe films grown on a W(100) substrate. Indeed there has been considerable work on the atomic structures and magnetic properties of these systems. Despite the lattice mismatch of about 9.4% between W and Fe, a much higher surface energy of the W(100) surface strongly favors monolayer nucleation for Fe films, and therefore, Fe films grow on the W(100) surface in a layer-by-layer basis with little interdiffusion.^{47,48} Magneto-optic Kerr effect measurements⁴⁸ suggest that films with thickness of around 1 monolayer are not ferromagnetic and are either nonmagnetic or antiferromagnetic. However, strong ferromagnetism is restored when a second Fe layer is added to the magnetically dead monolayer.^{47,48}

The results of our calculation of the local moments on each layer of the bcc-Fe_{*n*}/W(100) ($n \leq 8$) system in its paramagnetic state and the corresponding T_c 's along with the results for the bulk bcc-Fe for the same lattice parameter are presented in Table III and are consistent with these experimental findings. We note that, the local moment on the layer

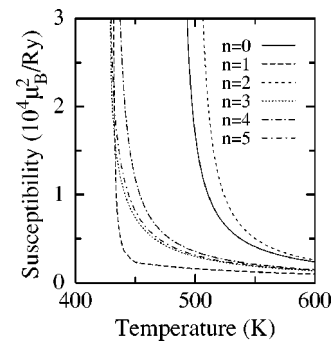


FIG. 4. Layer-diagonal paramagnetic spin susceptibility $\chi_{77}(\mathbf{q}_{\parallel}=0)$, for layer L_7 of the Cu_{*n*}/Fe₇/Cu(100) system for different overlayer thickness n as a function of temperature. The numbers in the legend imply the Cu overlayer thickness.

TABLE III. Local magnetic moments on different layers and the Curie temperatures of the $\text{Fe}_n/\text{W}(100)$ system. The layer L_1 is adjacent to the substrate and layer L_n is the topmost layer. The Fe monolayer on W(100) seems to be antiferromagnetic.

n	Local magnetic moments (μ_B)								T_c (K)
	L_1	L_2	L_3	L_4	L_5	L_6	L_7	L_8	
1	2.87								
2	2.19	3.22							969
3	2.41	2.78	3.14						1363
4	2.31	2.93	2.68	3.15					1484
5	2.33	2.88	2.83	2.69	3.15				1551
6	2.32	2.89	2.78	2.84	2.69	3.15			1595
7	2.32	2.89	2.79	2.79	2.84	2.69	3.15		1603
8	2.32	2.89	2.79	2.80	2.79	2.84	2.69	3.15	1642
Bulk	2.83								1687

adjacent to the W(100) substrate is about 30% smaller than that of the topmost layer (adjacent to the vacuum). The topmost layer has an enhanced local moment compared to that of the bulk. For thicker films ($n \geq 5$) the local moments on the layers inside the film are close to that of bulk bcc Fe.

In Table IV we present the effective “exchange parameters” $S_{PQ}^{(2)}(\mathbf{q}_{\parallel}=0)$, for the $\text{Fe}_7/\text{W}(100)$ system. We note that the intralayer parameter for layer L_1 which is close to the W(100) substrate is negative whilst it is positive for all other layers. This implies that the layer L_1 is antiferromagnetic and all other layers are ferromagnetic. The first nearest-neighbor interlayer coupling is always ferromagnetic. We also note that the interlayer coupling dies down rapidly after the first-nearest-neighbor layers. This feature is observed in all the films. Interestingly the exchange parameter for a single monolayer of Fe on W(100) is negative, and thus, the magnetic correlation in this layer is not ferromagnetic in agreement with the experimental observations.⁴⁸ When the film is capped by W overlayers the magnetic correlations in the topmost layer of Fe switches to antiferromagnetic, thus implying that the layer nearest to W is always antiferromagnetic.

To understand the electronic origin of this effect we plot the DOS in the L_1 [nearest to the W(100) substrate], L_4 (the middle layer), and L_7 (topmost layer) of the $\text{Fe}_7/\text{W}(100)$ in

Fig. 5. The DOS in the layer L_4 should be similar to the DOS of the bulk bcc-Fe for the same lattice parameter (5.98 a.u.) which is 9.4% larger than that of bcc-Fe. Because of the expansion in the atomic volume some of the states of the electrons with spin parallel to the local moment are pushed down from the Fermi energy resulting in more pronounced exchange splitting and an increase in the magnetic moment.⁴⁹ There is very little change in the DOS of the electrons with spin antiparallel to the local moment. The DOS in the topmost layer L_7 shows band narrowing due to a reduction in the coordination number. This also gives rise to a large local magnetic moment. These layers are all ferromagnetic. However, in the layer L_1 hybridization with W states at the interface cause some of the states of the electrons with spin antiparallel to the local moment near the Fermi energy to be transferred to the electrons with spin parallel to the local moment promoting the antiferromagnetic coupling between the local moments in this layer.

For $n \geq 2$ the system is ferromagnetic with T_c increasing monotonically as a function of film thickness, and approaching the value of T_c of the bulk bcc-Fe (with lattice parameter of W) at around $n=8$. Interestingly, the T_c 's in this case follow the empirical scaling law given by Eq. (4.1) with the scaling parameters $\lambda=1.6$, $n'=0.9$, and $n_0=0.9$. When the Fe films are capped by a single W monolayer the T_c is re-

TABLE IV. Intralayer $S_{PP}^{(2)}(\mathbf{q}_{\parallel}=0)$ and interlayer $S_{PQ}^{(2)}(\mathbf{q}_{\parallel}=0)$ ($P \neq Q$) effective exchange interaction in meV in the uncapped $\text{Fe}_7/\text{W}(100)$ system with the values for the $\text{Fe}_3/\text{W}(100)$ system given in parenthesis for comparison. The layer L_1 is adjacent to the W(100) substrate and layer L_7 (L_3) is the topmost layer.

Layers	L_1	L_2	L_3	L_4	L_5	L_6	L_7
L_1	-13.6(-14.9)	220(202)	-5.0(1.5)	1.5	1.9	-0.7	0.4
L_2	220(202)	67.5(49.7)	172(248)	2.8	-2.4	1.6	-0.7
L_3	-5.0(1.5)	172(248)	73.3(30.1)	177	5.3	-0.4	2.1
L_4	1.5	2.8	177	97.9	167	0.4	1.9
L_5	1.9	-2.4	5.3	167	69.3	175	7.9
L_6	-0.7	1.6	-0.4	0.4	175	45.0	262
L_7	0.4	-0.7	2.1	1.9	7.9	262	18.9

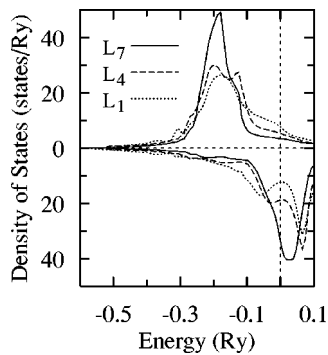


FIG. 5. Electronic density of states (DOS) in the layer nearest to the substrate (L_1), middle layer (L_4), and topmost layer (L_7) of the $\text{Fe}_7/\text{W}(100)$ system. The upper (lower) half of the figure shows the DOS for an electron spin-polarized parallel (antiparallel) to the local moment on a site. The energy is measured from the Fermi energy.

duced by about 150 K because the magnetic correlations in the topmost layer of Fe change from ferromagnetic to antiferromagnetic. Addition of another cap layer reduces the T_c further by 50 K and further additions make the T_c oscillate about this value, but the T_c never reaches the value of the uncapped film unlike the $\text{Fe}/\text{Cu}(100)$ and $\text{Co}/\text{Cu}(100)$ systems.

V. CONCLUSIONS

We have presented a first-principles electronic structure based theory to study the paramagnetic state of magnetic metallic thin films. A mean field DLM theory has been used to model the thermally induced spin fluctuations and there is a mutual consistency between this and the underlying locally exchange-split electronic structure. Within its framework we

have calculated the static paramagnetic spin susceptibility, and hence magnetic correlations, together with the Curie temperatures of fcc-Fe and fcc-Co films on $\text{Cu}(100)$ and bcc-Fe films on $\text{W}(100)$ substrates as a function of film thickness. The T_c 's of $\text{Fe}/\text{Cu}(100)$ and $\text{Co}/\text{Cu}(100)$ system are high for the films with single monolayer thickness but we expect our mean field theory to overestimate T_c significantly in this 2D limit. The T_c 's then decrease monotonically to the respective bulk values where the mean field estimates are expected and appear to be reasonable.¹² The intralayer magnetic correlations in these two systems are always ferromagnetic as well as the interlayer magnetic correlations in the $\text{Co}/\text{Cu}(100)$ system. In the $\text{Fe}/\text{Cu}(100)$ system the interlayer magnetic correlation for the top two layers is ferromagnetic and antiferromagnetic for the subsequent layers thereby making it a layered antiferromagnet below T_c . When these films are capped by Cu overlayers the T_c shows an oscillating behavior due to the change in the electronic structure near the interface. In the $\text{Fe}/\text{W}(100)$ system all the magnetic correlations are ferromagnetic except for the layers nearest to the $\text{W}(100)$ substrate or the W overlayer. This results in a reduction of the T_c when the films are capped by W overlayers.

ACKNOWLEDGMENTS

This work is a result of a collaboration under the TMR-Network (Contract No. ERBFMRXCT 96-0089) on "Ab initio calculations of magnetic properties of surfaces, interfaces, and multilayers" and also the RTN "Computational Magnetoelectronics" network (Contract No. HPRN-CT-2000-00143) and has been supported by the Engineering and Physical Sciences Research Council (UK) and the Hungarian National Science Foundation (Contracts No. OTKA T030240 and T038162).

*Present address: Dept. of Physics, Kuwait University, Safat 13060, Kuwait.

¹L.M. Falicov, D.T. Pierce, S.D. Bader, R. Gronsky, K.H. Hathaway, H.J. Hopster, D.N. Lambeth, S.S.P. Parkin, G. Prinz, M. Salamon, I.K. Schuller, and R.H. Victora, *J. Mater. Res.* **5**, 1299 (1990).

²M.T. Johnson, P.J.H. Bloemen, F.J.A. den Broeder, and J.J. de Vries, *Rep. Prog. Phys.* **59**, 15 409 (1996).

³H. Jenniches, J. Shen, C.V. Mohan, S.S. Manoharan, J. Barthel, P. Ohresser, M. Klaua, and J. Kirschner, *Phys. Rev. B* **59**, 1196 (1999).

⁴J. Hubbard, *Phys. Rev. B* **20**, 4584 (1979).

⁵H. Hasegawa, *J. Phys. Soc. Jpn.* **46**, 1504 (1979).

⁶D.M. Edwards, *J. Phys. F: Met. Phys.* **12**, 1789 (1982).

⁷A.I. Liechtenstein, M.I. Katsnelson, V.P. Antropov, and V.A. Gubanov, *J. Magn. Magn. Mater.* **67**, 65 (1987); M. van Schilf-gaarde and V.P. Antropov, *J. Appl. Phys.* **85**, 4827 (1999); M. Pajda, J. Kudrnovský, I. Turek, V. Drchal, and P. Bruno, *Phys. Rev. B* **64**, 174402 (2001).

⁸A.J. Pindor, J.B. Staunton, G.M. Stocks, and H. Winter, *J. Phys. F: Met. Phys.* **13**, 979 (1983).

⁹J.B. Staunton, B.L. Györfy, G.M. Stocks, and J. Wadsworth, *J.*

Phys. F: Met. Phys. **16**, 1761 (1986).

¹⁰B.L. Györfy, A.J. Pindor, J.B. Staunton, G.M. Stocks, and H. Winter, *J. Phys. F: Met. Phys.* **15**, 1337 (1985).

¹¹J.B. Staunton, B.L. Györfy, G.M. Stocks, and J. Wadsworth, *J. Phys. F: Met. Phys.* **15**, 1387 (1985).

¹²J.B. Staunton and B.L. Györfy, *Phys. Rev. Lett.* **69**, 371 (1992).

¹³E. Kisker, K. Schroder, M. Campagna, and W. Gudat, *Phys. Rev. Lett.* **52**, 2285 (1984).

¹⁴J. Kirschner, M. Globl, V. Dose, and H. Scheidt, *Phys. Rev. Lett.* **53**, 612 (1984).

¹⁵S. S. A. Razee, J. B. Staunton, L. Szunyogh, and B. L. Györfy, *Phys. Rev. Lett.* **88**, 147201 (2002).

¹⁶L. Szunyogh, B. Újfalussy, and P. Weinberger, *Phys. Rev. B* **51**, 9552 (1995).

¹⁷R. Zeller, P.H. Dederichs, B. Újfalussy, L. Szunyogh, and P. Weinberger, *Phys. Rev. B* **52**, 8807 (1995).

¹⁸K. Wildberger, R. Zeller, and P.H. Dederichs, *Phys. Rev. B* **55**, 10 074 (1997).

¹⁹For a review, see P. Weinberger and L. Szunyogh, *Comput. Mater. Sci.* **17**, 414 (2000).

²⁰R. Vollmer, S. van Dijken, M. Schleberger, and J. Kirschner, *Phys. Rev. B* **61**, 1303 (2000).

- ²¹M. Straub, R. Vollmer, and J. Kirschner, Phys. Rev. Lett. **77**, 743 (1996), and references therein.
- ²²M. Pajda, J. Kudrnovský, I. Turek, V. Drchal, and P. Bruno, Phys. Rev. Lett. **85**, 5424 (2000).
- ²³N.D. Mermin and H. Wagner, Phys. Rev. Lett. **17**, 1133 (1966).
- ²⁴R.P. Feynman, Phys. Rev. **97**, 660 (1955).
- ²⁵P. Weinberger, P.M. Levy, J. Banhart, L. Szunyogh, and B. Újfalussy, J. Phys.: Condens. Matter **8**, 7677 (1996).
- ²⁶S.S.A. Raze, J.B. Staunton, B. Ginatempo, E. Bruno, and F.J. Pinski, Phys. Rev. Lett. **82**, 5369 (1999).
- ²⁷S.S.A. Raze, J.B. Staunton, B. Ginatempo, E. Bruno, and F.J. Pinski, Phys. Rev. B **64**, 014411 (2001).
- ²⁸L. Szunyogh, B. Újfalussy, P. Weinberger, and J. Kollár, Phys. Rev. B **49**, 2721 (1994).
- ²⁹S.H. Vosko, L. Wilk, and M. Nusair, Can. J. Phys. **58**, 1200 (1980).
- ³⁰M. Hansen, *Constitution of Binary Alloys* (McGraw-Hill, New York, 1958).
- ³¹R. Germer, W. Dürr, W. Krewer, D. Pescia, and W. Gudat, Appl. Phys. A: Solids Surf. **47**, 393 (1988).
- ³²A. Dittschar, W. Kuch, M. Zharnikov, and C.M. Schneider, J. Magn. Magn. Mater. **212**, 307 (2000), and references therein.
- ³³S.S.P. Parkin, R. Bhadra, and K.P. Roche, Phys. Rev. Lett. **66**, 2152 (1991).
- ³⁴J. Mathon, M. Villeret, and H. Itoh, Phys. Rev. B **52**, R6983 (1995).
- ³⁵J.C.S. Kools, IEEE Trans. Magn. **32**, 3165 (1996).
- ³⁶L. Szunyogh, B. Újfalussy, U. Pustogowa, and P. Weinberger, Phys. Rev. B **57**, 8838 (1998).
- ³⁷F. Huang, M.T. Kief, G.J. Mankey, and R.F. Willis, Phys. Rev. B **49**, 3962 (1994).
- ³⁸S.Z. Wu, F.O. Schumann, G.J. Mankey, and R.F. Willis, J. Vac. Sci. Technol. **14**, 3189 (1996).
- ³⁹R.E. Camley and D. Li, Phys. Rev. Lett. **84**, 4709 (2000), and references therein.
- ⁴⁰T. Asada and S. Blügel, Phys. Rev. Lett. **79**, 507 (1997), and references therein.
- ⁴¹R.D. Ellerbrock, A. Fuest, A. Schatz, W. Keune, and R.A. Brand, Phys. Rev. Lett. **74**, 3053 (1995).
- ⁴²W.A.A. Macedo and W. Keune, Phys. Rev. Lett. **61**, 475 (1988).
- ⁴³J. Thomassen, F. May, B. Feldmann, M. Wuttig, and H. Ibach, Phys. Rev. Lett. **69**, 3831 (1992).
- ⁴⁴S. Müller, P. Bayer, C. Reischl, K. Heinz, B. Feldmann, H. Zillgen, and M. Wuttig, Phys. Rev. Lett. **74**, 765 (1995).
- ⁴⁵D. Li, M. Freitag, J. Pearson, Z.Q. Qiu, and S.D. Bader, Phys. Rev. Lett. **72**, 3112 (1994).
- ⁴⁶Ch. Wüsch, C.H. Back, L. Bürgi, U. Ramsperger, A. Vaterlaus, U. Maier, D. Pescia, P. Politi, M.G. Pini, and A. Rettori, Phys. Rev. B **55**, 5643 (1997).
- ⁴⁷R.L. Fink, G.A. Mulhollan, A.B. Andrews, J.L. Erskine, and G.K. Walters, J. Appl. Phys. **69**, 4986 (1991).
- ⁴⁸J. Chen and J.L. Erskine, Phys. Rev. Lett. **68**, 1212 (1992).
- ⁴⁹V. L. Moruzzi and P. M. Marcus, in *Handbook of Magnetic Materials*, edited by K. H. J. Buschow (Elsevier, Amsterdam, 1993), Vol. 7, p. 97.